Volume 4, Issue 5, 2020 ISSN: 2617-4537
DOI: https://doi.org/10.31058/j.data.2020.45001

Moving Target Indicator (MTI) RADAR Design Based on MATLAB/SIMULINK

Khine Thandar Soe[1*]

[1] Department of Electronic Engineering, Yangon Technological University, Yangon, Myanmar

Email Address

ecdepartment.ytu@gmail.com (Khine Thandar Soe)
*Correspondence: ecdepartment.ytu@gmail.com

Received: 8 August 2020**; Accepted:** 15 September 2020**; Published:** 24 September 2020

Abstract:

A pulsed Doppler radar is vulnerable to advanced repeat-back jamming techniques. Rapidly advancing technology producing inexpensive, high performance commercial off-the-shelf (COTS) components enable the construction of an electronic countermeasure (ECM) system capable of exploiting this vulnerability. This work addresses this threat by examining the nature of this vulnerability and developing a modification to the pulsed Doppler /MTI radar system. Pulsed Doppler radar systems use pulse compression waveforms such as pseudo noise (PN) coded binary phase-modulated sequences. Repeat-back jamming listens, stores, and repeats back the radar's transmitted signal to block out all other return signals. If a different PN-code is used for each pulse, the radar receiver will be minimally affected by the jamming. However, a varying PN code creates range side lobe variation that degrades the integrated signal-to-clutter ratio by a factor of 1/N2 where N is the code length. This severely limits the ability to perform Doppler and Moving-Target Indication (MTI) processing for clutter suppression on the radar return. To recover this performance loss several receiver filtering and digital signal processing techniques are tested. PN code selection for optimum filter performance is explored resulting in a 7-dB signal-to-clutter performance recovery for a 32-bit code. Digital pulse compression, matched filtering, and adaptive digital equalization filtering methods are applied to the radar return to equalize differences created by variable PN codes. Different equalization algorithms with various subsets of PN-codes are presented and simulated with data sets modeled after existing radar systems. Successful correction reduces clutter, minimizes the performance degradation to MTI due to variable pulse-codes.

Keywords:

Moving Target Indicator (MTI), RADAR, Numerical Analysis, MATLAB, SIMULINK

1. Introduction

Radar systems in hostile environments face the challenge of detecting targets in the midst of noise, clutter, and jamming. The magnitudes of these interference signals are typically many times that of the target signal. Many techniques have been developed to mitigate this interference and extract the target's parameters. Two classes of radar

systems designed for this purpose are the moving target indication (MTI) radar and the pulsed Doppler (PD) radar. Both systems utilize the Doppler Effect to separate moving targets from relatively stationary clutter. Clutter typically consists of unwanted radar reflections after the sea, terrain, weather, or chaff. MTI and PD radars are widely used and play a critical role in many modern radar systems. Civilian systems rely on MTI and PD radar for air surveillance, especially in bad weather. Military applications include the detection of low flying aircraft or missiles from shipboard and airborne radar platforms [1,2].

Military radar systems often operate in hostile environments and may be targeted by electronic countermeasures (ECM) such as repeat-back or digital radio-frequency memory (DRFM) jamming. DRFM jamming captures radar signals to amplify and repeat-back to the radar to flood the receiver with erroneous data. Advances in technology have made inexpensive, high-performance radio frequency parts available so that a DRF jamming system can easily be developed to blind a PD radar. This work addresses this threat by examining the nature of this vulnerability and developing a modification to the pulsed Doppler MTI radar system to resist some forms of DRFM jamming.

Moving Target Indication (MTI) Radar is an older system that uses delay-line cancellers to filter out clutter. The current radar return is compared with previous returns to isolate differences. The relatively stationary clutter is subtracted out and moving targets remain. A newer implementation of MTI modifies t IH' pulsed Doppler radar return by adding a notch filter around the Doppler frequencies of the clutter in order to improve the signal-to-clutter ratio [3,4].

There is a significant performance loss in the ability to Doppler process or apply an MTI filter to the return of a variable pulse-code radar. The performance loss was found to be the result of clutter range side lobe variation. This work presents several receiver filtering methods by which this performance may be recovered. A simulation framework and graphical user interface created for PD and MTI radar simulation will be presented. The signal-to-clutter ratio degradation of the return when using variable code sets and matched filtering will be quantified. Pulse compression is explored as an alternative. However, pulse compression filters do not meet the signal-to-noise ratio (SNR) optimality criteria of matched filtering. Adaptive digital equalization filtering methods are applied to the' matched filter output to attempt to recover PD and MTI performance. The SNR loss of applying the equalization filter will be compared with the SNR loss of a pulse compression filter. Pulse code selection for maximum filter performance and weighting techniques for further performance improvements will be explored. Finally the effect of jamming on constant and variable pulse-code sequences will be shown to test the success of the variable pulse-code radar solution to repeat-back jamming.

2. Moving Target Indicator Radar System

MTI filters can be implemented using delay line cancelers. The frequency response of this class of MTI filter is periodic, with nulls at integer multiples of the PRF. Thus, targets with Doppler frequencies equal to nf_r are severely attenuated. Since Doppler is proportional to target velocity ($fd = nv / \lambda$), target speeds that produce Doppler frequencies equal to integer multiples of are known as blind speeds. Radar systems can minimize the occurrence of blind speeds by either employing multiple PRF schemes (PRF staggering) or by using high PRFs where in this case the radar may

become range ambiguous. The main difference between PRF staggering and PRF agility is that the pulse repetition interval (within an integration interval) can be changed between consecutive pulses for the case of PRF staggering.

The block diagram of coherent MTI radar is shown in Figure.1. The coherent transmission is controlled by the STAble Local Oscillator (STALO). The outputs of the STALO, f_{LO}, and the COHerent Oscillator (COHO),f_C, are mixed to produce the transmission frequency, $f_{LO}+ f_C$. The Intermediate Frequency (IF), $f_C \pm f_d$, is produced by mixing the received signal with f_{LO}. After the IF amplifier, the signal is passed through a phase detector and is converted into a base band. Finally, the video signal is inputted into an MTI filter [5,6,7].

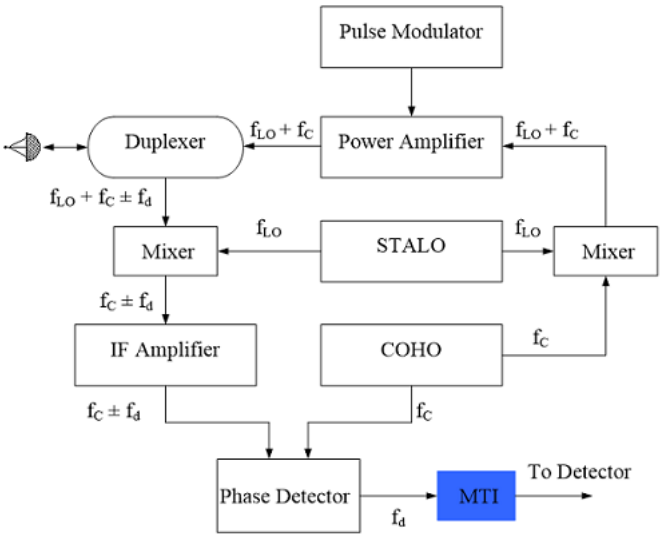

Figure 1. *Block Diagram of Coherent MTI Radar.*

3. Receiver Implementation and Performance Bounds

The incoming received signal was sampled at times T_0, T_1 .., T_{N-1}-and weighed by a complex vector w of (N×1) dimensions. The resultant input is then given by

$$r = c + s(\theta) \tag{1}$$

where r, c, s(θ) are N × 1 column vectors representing the received signal, the clutter echo, and the target echo, respectively, the last being a function of a random phase 0.

The filter average output power, averaged over the clutter and the random phase is

$$P_0 = \frac{1}{2} E\{|w^*[c + s(\theta)|^2\} \tag{2}$$

$$P_0 = \frac{1}{2} E\{w^*cc^*w\} + \frac{1}{2} E\{w^*s(\theta)s^*(\theta)w\} + E\{Re[w^*cs^*(\theta)w]\} \tag{3}$$

where E{*} is the expectation operator and an asterisk denotes transpose conjugate. The last term in (2) is zero for uncorrelated clutter and target echo.

The clutter was characterized by a wide sense stationary, zero mean, complex Gaussian random process with a covariance matrix given by

$$\frac{1}{2} E\{cc^*\} \triangleq C_0 K \tag{4}$$

where C_o is a constant related to clutter radar cross section and K is the normalized clutter covariance matrix. Then the output power of target echo

$$P_{t_0}=\frac{1}{2}w^*E\{s(\theta)s^*(\theta)\}w \tag{5}$$

the output power of clutter echo

$$P_{C_0}=C_0w^*Kw \tag{6}$$

the input power of target echo

$$P_{t_i}=\frac{1}{2}w^*E\{s(\theta)s^*(\theta)\} \tag{7}$$

and the input power of clutter echo

$$P_{C_i}=C_0 \tag{8}$$

The output signal to clutter ratio (SCR) is then

$$(SCR)_0=\frac{1}{2}w\,^*E\{s(\theta)s^*(\theta)\}w/C_0w^*Kw \tag{9}$$

and the input SCR

$$(SCR)_i=\frac{1}{2}E\{s(\theta)s^*(\theta)\}/C_0 \tag{10}$$

The MTI gain or "improvement factor" is therefore

$$G=\frac{(SCR)_0}{(SCR)_i}=\frac{\frac{1}{2}w\,^*E\{s(\theta)s^*(\theta)\}w/C_0w^*Kw}{\frac{1}{2}E\{s(\theta)s^*(\theta)\}/C_0}=\overline{G}.F(s) \tag{11}$$

where $\overline{G}$ represents the average value and where $\overline{G}$ w*w/w*Kw is the "reference gain" [5], independent of signal characteristics and

$$F(s)=\frac{w\,^*E\{s(\theta)s^*(\theta)\}w}{w^*w\,E\{s(\theta)s^*(\theta)\}} \tag{12}$$

is the so-called "signal shape factor" [1]. The resultant receiver is depicted in Figure 2 and consists of an in-phase (I) channel and a quadrature (Q) channel designed to eliminate the system dependence on the random echo phase 0 ("blind phase" [7]). The low-pass filters cover the Doppler domain of interest and are utilized in order to increase the system noise immunity.

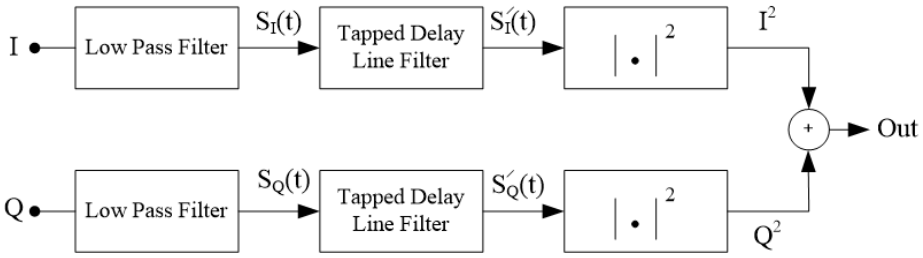

***Figure 2**. Coherent Quadrature Channel Receiver.*

For such a system it can be readily shown [7], that if we assume a target Doppler domain given by $[f_{tL}\ ;\ f_{tH}]$, such that $(f_{tH}-f_{tL})\ (T_{i+1}-T_i) > 1$, for all i, and the average filter power transfer ratio is

$$F(s)=H_{p(f)}=\sum_{i,k=1} w_iw_k^*\exp\text{-}j2\pi f(T_i-T_k) \tag{13}$$

over the a priori probability density function of target Doppler shifts, the MTI gain becomes

$$G(f)\cong\overline{G}=w^*\,w/w\,^*Kw \tag{14}$$

A system optimized on the basis of the MTI gain may result in a signal shape factor which could deteriorate the overall system performance. This stems from the fact that F(s) favors certain Doppler frequencies over others. This penality is incurred in introducing an optimization criterion independent of the signal characteristics (Doppler shift). It also means that, as far as false alarm rate and detection probability are concerned, one can no longer make any a priori judgement of whether the system detection performance is satisfactory, since the target Doppler may fall anywhere within the anticipated target Doppler domain.

A desirable signal shape factor, F(s) = 1, requires a constant maximum gain of the tapped delay line filter over the passband, implying total elimination of blind speeds. This also implies that for an optimized stagger code the signal shape factor automatically attains its optimum value under the circumstances.

The expression for the reference gain in (14) can be recognized as the reciprocal of the Rayleigh quotient. This implies that

$$\overline{G}_{max} = \max_w\{w^* w / w^* K w\} = \frac{1}{\lambda_{min}} \tag{15}$$

where λ_{min} is the smallest eigenvalue of K and w its corresponding eigenvector ($w^*w = 1$). This also implies that

$$1/\lambda_{max} \le \overline{G}_{max} \le 1/\lambda_{min} \tag{16}$$

Assuming a normalized clutter power spectrum density function of the familiar form

$$|C(f)|^2 = \left(1/\sqrt{2\pi}\sigma_C\right)\exp-\frac{f^2}{2\sigma_C^2} \tag{17}$$

where σ_C^2 is the variance of clutter Doppler shift, the output clutter power is easily formulated as [7]

$$P_{C_O} = w^* K w \tag{18}$$

where K is the normalized clutter covariance matrix whose elements are given by

$$K_{ij} = \begin{cases} \exp-2\pi^2\sigma_C^2(T_i - T_j)^2, & i \neq j \\ 1, & i = j \end{cases} \tag{19}$$

As can be seen, P_{C_O} results in a positive definite Hermitian form (since K is a positive definite Hermitian matrix). The eigenvalues of K are therefore real, positive, and distinct. It can also be seen for $T_{i+1} - T_i = T$ for all i that K is a Toeplitz matrix. From the above it can be shown that the minimum eigenvalue of K is bounded by

$$0 \le \lambda_{min} \le 1 \tag{20}$$

Based on this the following bounds have been shown [6,7] for a constant PRF system with period T

$$\lambda_{min}^{(N+1)} \le \lambda_{min}^{(N)} \tag{21}$$

where (N+1) and (N) refer to (N+1) X (N+ 1) and N ×N matrices, respectively, and therefore:

$$\overline{G}_{max}^{(N+1)} \ge \overline{G}_{max}^{(N)} \tag{22}$$

or in other words the optimum reference gain will increase with an increase in the number of processed pulses. Due to this and the asymptotic properties of Toeplitz matrices $\overline{G}_{max}$ attains a bound as $N \longrightarrow \infty$. This implies that there exists a practical bound on the number of processed pulses. Calculations indicate that for σ_C = 0. 1, 20 pulses provide an additional improvement of less than 3 dB in reference gain over 10 pulses. As a, increases to large values (i.e., the clutter Doppler spread becomes large), the value of the reference gain is independent of the number of processed pulses, or

$$\lambda > 1 - \frac{1}{2}\exp -2\pi^2\sigma_C^2 T^2 \tag{23}$$

in the limit where $\sigma_C \longrightarrow \infty$, $\lambda = 1$, which actually represents the "white noise" case.

The system was optimized for a given standard deviation of clutter Doppler σ_O, resulting in a set of weights $w(\sigma_O)$. Then, if the input clutter has standard deviation a, such that $\sigma < \sigma_O$, the output clutter power will decrease. If $\sigma > \sigma_O$ the output clutter will increase. In other words,

$$\lambda[\sigma, w(\sigma_0)] < \lambda[\sigma_0, w(\sigma_0)], \sigma < \sigma_0 \tag{24}$$

and by the definition of minimum eigenvalues

$$\lambda[\sigma, w(\sigma)] < \lambda[\sigma 0, w(\sigma 0)] \tag{25}$$

This is widely known as the monotonic property [7] and is illustrated in Figure 3. Based on the above bounds for the case of a constant PRF system, the following can be shown [5] for a staggered PRF system.

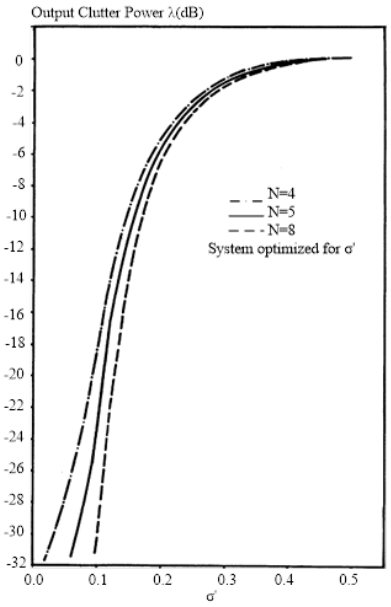

Figure 3. *The Monotonic Property.*

Given a staggered system of pulse intervals such that

$$T^{(-)} \triangleq T_{min} \leq T_{i+1} - T_i \leq T_{max} \triangleq T^{(+)} \tag{26}$$

for all I, so that

$$T^{(+)} = (1 + \alpha)T^{(-)}, 0 < \alpha < 1 \tag{27}$$

the performance of this system will be bounded by two constant PRF systems, one with interpulse spacing equal to $T^{(-)}$, the other with interpulse spacing equal to $T^{(+)}$. In other words

$$\lambda_{min}^{(-)} \leq \lambda_{m}^{(s)} \leq \lambda_{min}^{(+)} \tag{28}$$

4. Implementation and Results

The flowchart for simulation based on the radar signal processing is shown in Figure 4. There are many input parameters to simulate with many moving targets. The noise level, range, azimuth, measurement parameters and target are declared for input section. And then the range Doppler algorithm is activated according to the input parameters. The range and azimuth compression are evaluated and their responses are easily demonstrated based on the target model.

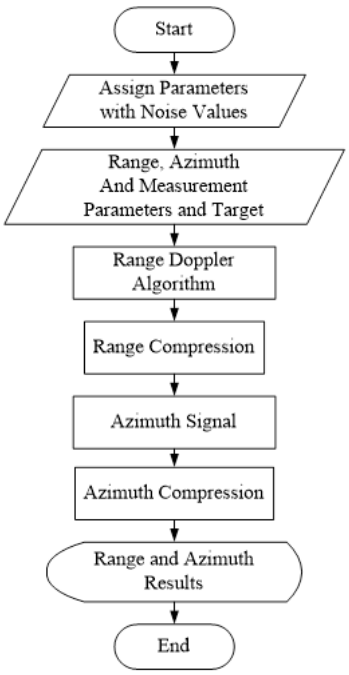

Figure 4. *Flowchart for Simulation.*

There are two simulation approaches for radar signal processing. The first one is for worst case condition and the second one is for optimum condition. The input image (.gif format) could be exchanged by Doppler algorithm and then inputted to the processing unit. The optimum condition for radar signal processing is clearer than the worst case condition image.

The SIMULINK model for MTI system for Radar Signal Processing is illustrated in Figure 5. The radar receiver front end is the heart of the implemented system design. The operation of each block sets is to evaluate the performance of the MTI process for Radar Signal Processing. The functional flowchart for SIMULINK model design is also mentioned in Figure 4. Based on the theoretical approach to MTI system, the details implementation is described. The moving targets are processed by using radar pulse generation. All units are operated by applying the virtual unit for experimental setup in Radar Signal Processing with the help of MATLAB/SIMULINK.

Volume 4, Issue 5, 2020 ISSN: 2617-4537
DOI: https://doi.org/10.31058/j.data.2020.45001

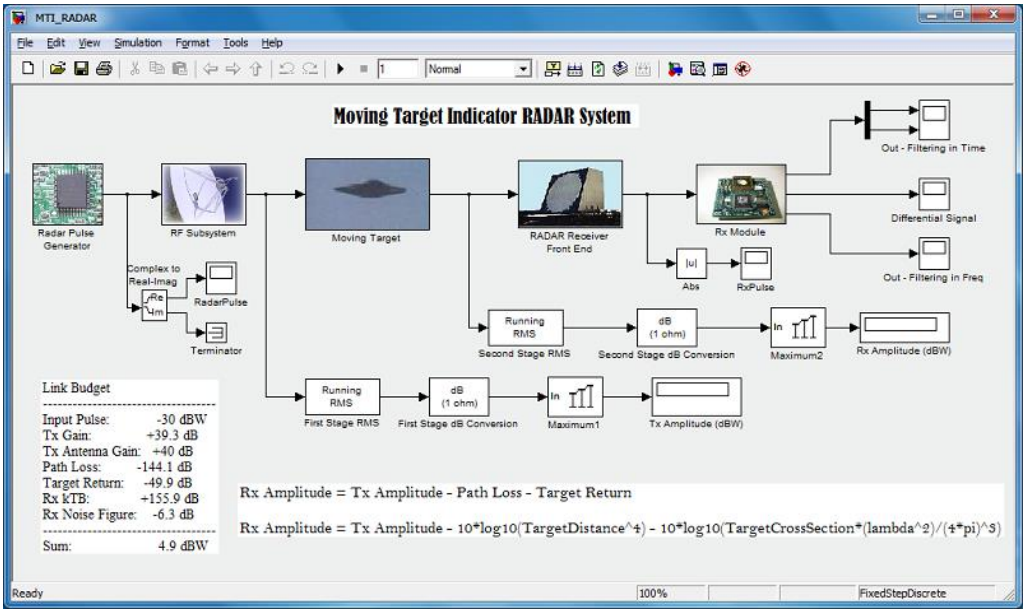

Figure 5. *SIMULINK Model for Proposed Design.*

5. Radar Return for a Burst of LFM Pulses

The analysis for radar return for a burst of LFM pulses is illustrated in Figure.6. This analysis is based on the usage of MTI implementation and matched filter for radar simulation process. The initial pulses are lapped by comparing with the return pulses for radar simulation analysis. The domain for analysis of radar return for a burst of LFM pulses is based on the time. It is developed by the supported sub functions for pulse analysis.

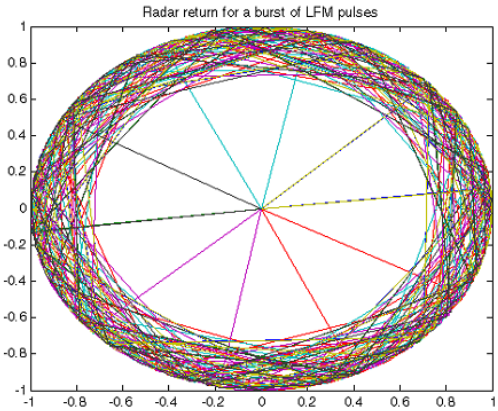

Figure 6. *Radar Return for a Burst of LFM Pulses.*

6. Simulation Results from MTI SIMULINK Model

The simulation results from MTI radar SIMULINK model are mentioned in this section. The radar pulse generator generates the radar pulse to find the moving target. These radar pulses are illustrated in Figure 7. The period for the radar pulse signal is between 0 to 1 second and the sample period is approximately 0.1 second. These pulses can strike to the moving target and the return pulses could also be emitted from these moving target. The received pulse could also be monitored on the radar monitor. The received radar pulse signals from moving target are mentioned in Figure 8.

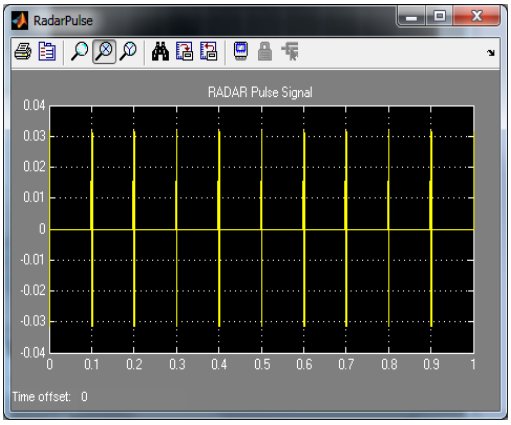

Figure 7. *Screenshot Result for Radar Pulse Signal.*

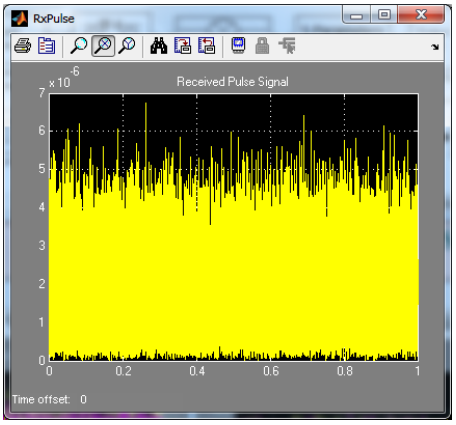

Figure 8. *Received Pulse Signal from Moving Target.*

The magnitude response and phase response from RF module are illustrated in Figure 9. These two responses with respect to time for MTI radar simulation system depend only on the size and shapes of the moving target and its position. These responses say the equal amount of real time simulation results from moving target by comparing with the actual simulation action. The phase response from RF module says the linear model approach results for moving target.

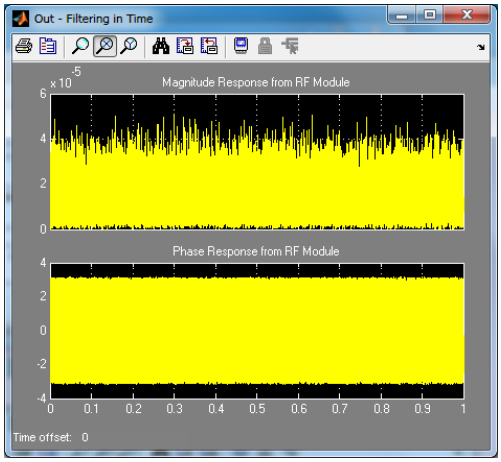

Figure 9. *Screenshot Result for Magnitude and Phase Responses from RF Module.*

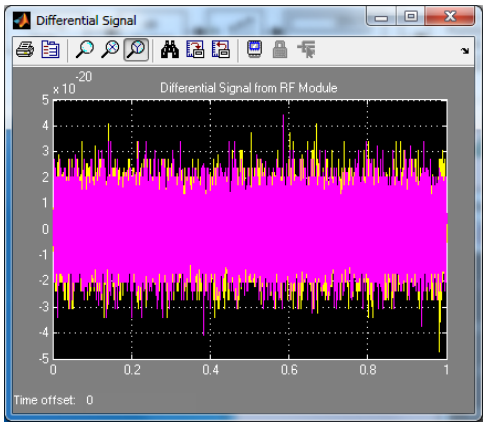

Figure 10. *Screenshot Result for Differential Signal from RF Module.*

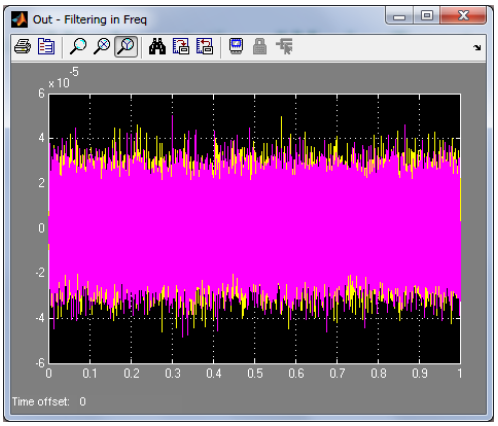

Figure 11. *Screenshot Result for Filtering in Frequency Domain.*

The screenshot result for differential signal from RF module is shown in Figure.10. This response says the difference between the transmitted and received signal for moving target via MTI radar system. The yellow one is for transmitted signal pulses and the pink one is for received signal pulses from the moving target. The screenshot result for filtering in frequency domain is illustrated in Figure 11. The yellow one is for transmitted signal pulses and the pink one is for received signal pulses from the moving target.

7. Simulation Results for UAV Images

The specified target for MTI radar system analysis is only UAV and the range is evaluated according to the specified parameters of the implementation. The best condition of MTI for moving target (UAV) is illustrated in Figure 12 to Figure 15. The target image is clear and the image matrix is satisfied to get the input of the MTI radar unit.

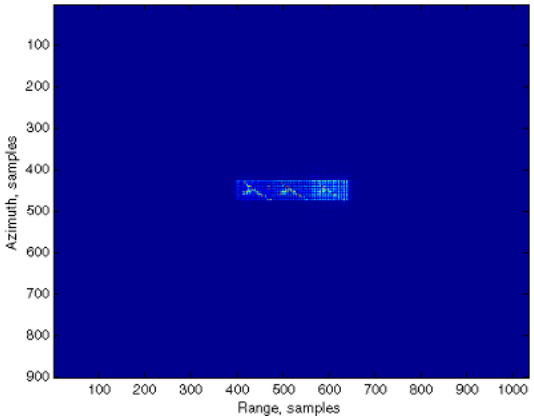

Figure 12. *Best Condition of MTI for Moving Target (UAV Image1).*

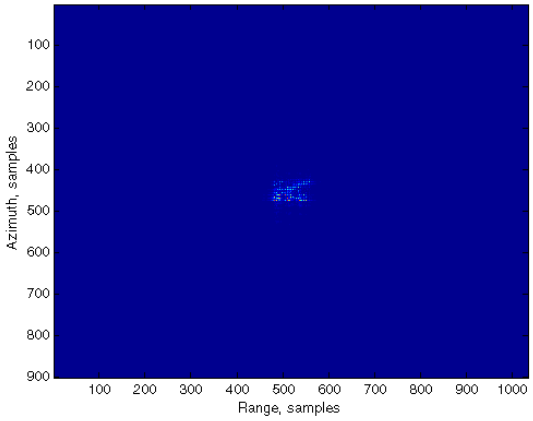

Figure 13. *Best Condition of MTI for Moving Target (UAV Image2.)*

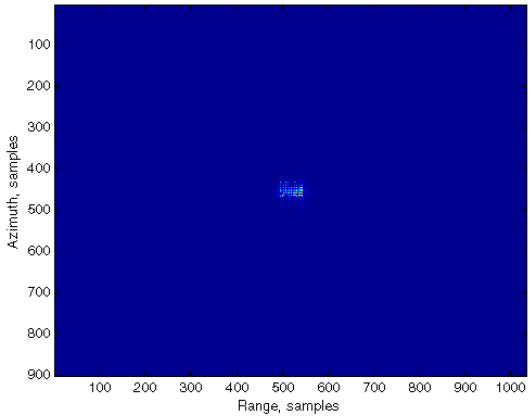

Figure 14. *Best Condition of MTI for Moving Target (UAV Image3).*

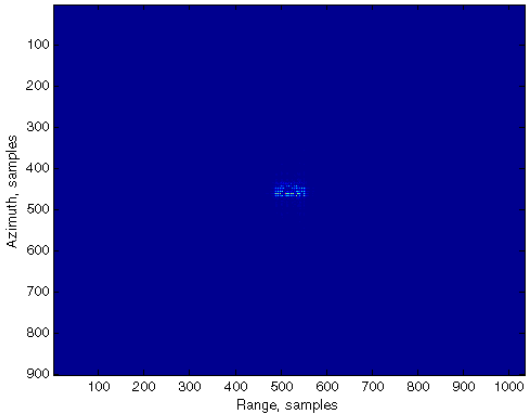

Figure 15. *Best Condition of MTI for Moving Target (UAV Image4).*

8. Statistic Information of Detection

The statistic information of detection for various types of UIAV model is mentioned in Table 1. The detection times for various UAV model are between 10 to 15 minutes for resolution of each images. The accuracy of detection depends only on the ratio of original image resolution to the detected image resolution.

Table 1. *Statistic Information for Various UAV Model.*

UAV Name	UAV Model	Detection Time by MATLAB	Accuracy
UAV1		~ 15 Minutes	90%
UAV2		~ 10 Minutes	85%
UAV3		~ 12 Minutes	85%
UAV4		~ 10 Minutes	83%

9. Conclusion

In this work, a new modification to the Pulsed Doppler and Moving Target Indication radar systems was explored. The variable pulse-code radar system was proposed in response to a potential vulnerability to repeat-back jamming in current systems. This new system varies the codes within coherent processing intervals by changing the PN code sequence transmitted with each PRI. This is highly effective in resisting some types of repeat-back jamming. However, the use of variable pulse-codes results in a significant performance loss in the ability to Doppler process or applies an MTI filter to the return. The performance loss was investigated and it was discovered that while the zero-lag peak values of the return signal were unaffected by using variable pulse-codes, there was a significant amount of clutter side lobe interference during matched filtering. The pulse compression filter was successful due to the absence of side lobe energy in the filtered output. However, the pulse compression filter suffers from a 2.5 dB SNR loss when compared to the matched filter. Further filtering of codes was performed by examining time responses of the reciprocal spectrum of code sequences to create a subset of 32-bit codes which optimized the pulse compression filter. The maximum SNR matched filter was revisited with the addition of adaptive digital equalization filters designed to recover pulsed Doppler and MTI performance based on the lessons learned previously. A flat spectrum equalization filter, similar in function to the pulse compression filter, was tested and found to be successful in recovering some Doppler performance. To attempt to combine the advantages of the matched filter and pulse compression filter was designed to maximize Doppler performance using variable pulse-codes. This too was found to be successful. Finally, the variable pulse-code radar has met its performance goals in this thesis and shows promise for future development.

Conflicts of Interest

The author declares that there is no conflict of interest regarding the publication of this article.

Funding

This research received no specific grant from any funding agency in the public, commercial or not-for-profit sectors.

References

[1] Skolnik, M. Radar handbook, Second Edition, McGraw-Hill, USA, 1970; pp. 1-846, ISBN 0-07-057913-X.

[2] Skolnik, M. Introduction to Radar Systems, Third Edition, McGraw-Hill, USA, 1980; pp. 1-784, ISBN-13: 978-0072881387.

[3] Yang, J. Study on Ground Moving Target Indication and Imaging Technique of Airborne SAR, First Edition, Springer, Singapore, 2017; pp. 1-122, ISBN 13: 978-981-10-3075-8.

[4] Sorrell, P.A. Microwave systems design for high-performance moving target indicators in radars. *IEEE Transactions on Microwave Theory and Techniques*, 1991, 39(5), 791-797.

[5] J.W. Taylor, Jr., in Radar Handbook, M.I. Skolnik, Ed. New York: McGraw-Hill, 1990, ch. 3.5.

[6] Sorrell, P.A. Radar stability self test using bulk acoustic wave delay lines. *Proc. 9th IEEE 44th Annual Frequency Control Symp.*, 23-25 May 1990, DOI: 10.1109/FREQ.1990.177494, Baltimore, MD, USA.

[7] Sorrell, P.A. Review of radar stability needs and problems, presented at 1990 Asia Pacific Microwave Conf.-APMC '90, September 18-21, 1990 Sunshine City Prince Hotel and World Import Mart Building, Tokyo, Japan.